Journal of Photochemistry and Photobiology A: Chemistry 288 (2014) 70–75

Contents lists available at ScienceDirect

Journal of Photochemistry and Photobiology A: Chemistry

journal homepage: www.elsevier.com/locate/jphotochem

Enhanced charge transfer character of photoexcited states of dye sensitizer on the N719/TiO_2 interface as revealed by electroabsorption spectra

Kamlesh Awasthi [a], Hung-Yu Hsu [b], Eric Wei-Guang Diau [b,*], Nobuhiro Ohta [a,*]

[a] Research Institute for Electronic Science, Hokkaido University, Sapporo 001-0020, Japan
[b] Department of Applied Chemistry and Institute of Molecular Science, National Chiao Tung University, Hsinchu 30010, Taiwan

ARTICLE INFO

Article history:
Received 25 February 2014
Received in revised form 17 April 2014
Accepted 1 May 2014
Available online 13 May 2014

Keywords:
Dye sensitized solar cell
TiO_2
Ruthenium complex
Electroabsorption spectrum
Interfacial electron transfer

ABSTRACT

Electroabsorption (E-A) spectra of $(Bu_4N)_2[Ru(dcbpyH)_2(NCS)_2]$ (N719) sensitized on TiO_2 nanoparticles are very different from those of the N719 solid film. In contrast with N719 fixed in a solid form, N719 adsorbed on TiO_2 shows a significant electric field effect on absorbance, indicating the strong interaction in the surface between N719 and TiO_2. The magnitude of the change in electric dipole moment following absorption of N719 sensitized on TiO_2 is much greater than that of the sold film, suggesting that the interfacial charge transfer occurs following photoexcitation of N719 adsorbed on TiO_2 surface.

1. Introduction

Dye-sensitized solar cells (DSSC) are considered as a strong alternative to conventional photovoltaic devices that used semiconductors, such as silicon. The advantages of DSSC are their high efficiency, simple fabrication process and low cost production [1]. Numerous sensitizers including rutheniums complexes [2–6], metal-free organic dyes [7–9], and porphyrin dyes [10,11] are employed in DSSC devices. In any DSSC device, efficient electron injection from the excited state of dye sensitizers to the conduction band (CB) of nanocrystalline titanium dioxide (TiO_2) is essential. To design and develop more efficient and stable organic devices, deep understanding of photoexcitation dynamics of these dye sensitizers attached on TiO_2 is essential.

Among ruthenium complexes, Ru(II) polypyridal complex dyes adsorbed on TiO_2 have been the main subject, and bis(tetrabutylammonium)-cis-di(thiocyanato)-N,N′-bis(4-carboxylato-4′-carboxylic acid-2,2′-bipyridine)ruthenium (II) (N719) is a typical complex, which gives the energy conversion efficiency over 11% with the liquid I^-/I_3^- electrolyte [12]. The metal to ligand charge transfer (MLCT) promotes an electron from the metal center to a ligand that is directly bound to the semiconductor surface [13].

The ultrafast electron injection occurs after light absorption of the MLCT band, and the injection time has been estimated to be as fast as 10–25 fs for the ruthenium complexes containing 4,4′-dicarboxyl-2,2′-bipyridine ligand, i.e., N719 and cis-bis(4,4′-dicarboxyl-2,2′-bipyridine)-bis(isothiocyanato)-ruthenium(II), i.e., N3 [14–16]. According to the theory for excited-state electron injection into wide-bandgap semiconductor, the rate of interfacial electron transfer at an electrode surface depends critically on the overlap of the sensitizer excited state distribution function with the semiconductor density of states [17]. To obtain the extremely fast electron injection, strong electronic coupling between photoexcited sensitizer and semiconductor should be generated through the anchoring groups of the dye, along with a high density of CB states of the semiconductor surrounding the excited state of the dye.

The adsorption geometry of N719 on extended TiO_2 modes was calculated using a systematic density functional theory [18]. The energy levels of the excited state of N719 relative to the CB of TiO_2 as well as the electronic coupling between the attached dye, i.e., N719, and TiO_2 were also calculated. The results indicated that the visible absorption band centered at ~530 nm corresponds to the transition to the combined system's excited state having strong coupling between dye and TiO_2, that is, the electron injection occurs following optical transition from the ground state of the dye to an

* Corresponding author.
E-mail addresses: diau@mail.nctu.edu.tw (E.W.-G. Diau), nohta@es.hokudai.ac.jp (N. Ohta).

http://dx.doi.org/10.1016/j.jphotochem.2014.05.001
1010-6030/

excited state largely delocalized within the semiconductor [19]. If this is the case, the electric dipole moment is expected to be very large at the excited state of N719 sensitized on the surface of TiO_2, in comparison with those of N719 without TiO_2.

Electroabsorption and electrophotoluminescene spectroscopies, where electric field effects on absorption and photoluminescence spectra are measured, are powerful techniques to investigate the charge separated character of the excited state because the change in electric dipole moment following optical transition can be determined. In fact, these techniques have been applied to dye sensitizers attached to TiO_2 to evaluate the charge-separated character of the photoexcited state [20–24]. Interestingly, the local electric field induced by the photoinduced electron transfer of sensitizers attached to TiO_2 has been also discussed by comparing the electroabsorption spectra observed with and without photoirradiation [24–26].

In the present study, we have measured electroabsorption (E-A) spectra of N719 adsorbed on TiO_2 nanoparticles in a thin-film condition similar to that used in DSSC, along with the E-A measurements of N719 solid films. For both samples, we analyzed the E-A spectra, and the magnitudes of the change in electric dipole moment, molecular polarizability and transition moment following photoabsorption have been evaluated. Based on the results, the mechanism of the electron injection in the N719/TiO_2 interface has been discussed.

2. Experimental

Commercially available N719 (Everlight Chem. Ind. Corp., Taiwan) was used without further purification. Two kinds of samples of N719, i.e., samples (I) and (II), were prepared. Sample (I), which is the N719 thin solid film, was prepared by deposition of N719 dye on an indium-tin-oxide (ITO) coated quartz substrate by a spin-coating method from ethanol solution. Poly(methyl methacrylate) (PMMA) film was deposited on the N719 solid film. Sample (II), which was the film composed of TiO_2 and N719, was prepared by using a standard method reported elsewhere [5]. A paste composed of TiO_2 nanoparticles (size ~15 nm) was coated on a $TiCl_4$-treated FTO glass substrate with one screen-printing layer. After a programming sintering process, the post-treatment of $TiCl_4$ was imposed to the TiO_2 film (thickness 3.5 μm) and sintered again at 500 °C for 30 min. After cooling in air, the sintered TiO_2 films were immersed into N719 dye solution (0.3 mM in acetonitrile and tert-butanol with equal volume ratio) at 25 °C for 2 h for dye loading onto the surface of TiO_2. After solvents were evaporated, a PMMA film was deposited on the N719/TiO_2 films by the spin-coating method. In both samples (I) and (II), the thickness of PMMA films was typically 0.5 μm, which was measured with an interferometric microscope (Nano Spec/AFT010-0180, Nanmetric). A semitransparent aluminum film (Al) was deposited on the PMMA films in both samples by a vacuum vapor deposition technique. ITO or FTO and Al were used as electrodes in the electroabsorption (E-A) measurements. Since N719 on the surface of TiO_2 is covered by a PMMA film in sample (II), it is not necessary to consider the desorption of N719 from the TiO_2 surface during the optical measurements.

Polarized E-A spectra were measured with electric-field modulation spectroscopy under atmospheric conditions with magic angles between the direction of applied electric field and the electric vector of the excitation light [27]. A convergent light beam from the xenon lamp of JASCO FP-777 spectrometer was collimated with a pinhole having a diameter of 1.4 mm and with a lens having focal length 20 mm and directed through a 10 mm aperture α-barium borate (BBO) polarization prism and through the sample slide to an external photomultiplier. A rotator stage was used for varying the angle between the polarization direction of the excitation light and the direction of applied field. A signal from the photomultiplier was amplified and divided into two channels. The DC component directly collected with a computer, and the ac component synchronized with the applied ac voltage was recorded with a lock-in amplifier (SR830, SRS). The amplitude and phase signals from the output of lock-in amplifier at the second harmonic of the modulation frequency ($\Delta I(2\nu)$) were digitized and recorded, together with the dc component of transmitted light intensity. The change in absorption intensity, i.e., ΔA, caused by the applied electric field is defined as $\Delta A = -(2\sqrt{2}/\ln 10)\Delta I(2\nu)/I$ where the factor $2\sqrt{2}$ converts the value of measured rms signal to its equivalent dc signal, I and ΔI represent the transmitted light intensity and its field-induced change, respectively.

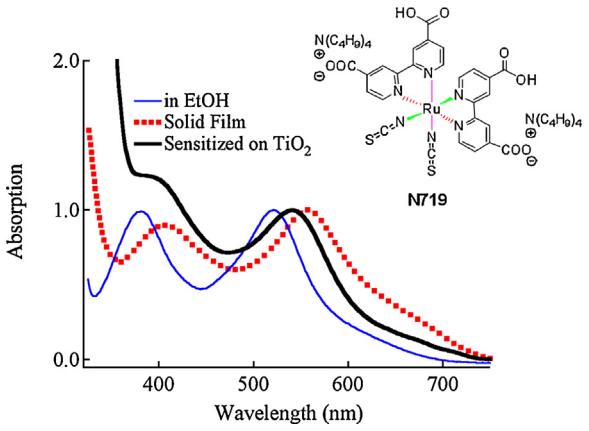

Fig. 1. Absorption spectra of N719 in ethanol (thin solid line), in crystal (dotted line, sample (I)) and on TiO_2 particles (thick solid line, sample (II)). The absorption intensity is normalized to unity at the peak around 500–600 nm.

3. Results and discussion

Fig. 1 shows the absorption spectra of N719 dye under different conditions. The absorption spectra of N719 in ethanol solution shows bands having a peak at 521 and 381 nm, which are hereafter denoted by Bands 1 and 2, respectively. These bands are assigned to the metal-to-ligand charge transfer (MLCT) bands, and their locations depend significantly on the environment. For example, Band 1 is red-shifted by 36 and 22 nm, respectively, in sample (I) and in sample (II), respectively, in comparison with the corresponding band in ethanol (see Table 1). The N719/TiO_2 surface is covered by a PMMA film in sample (II), and the N719 thin solid film is also covered by a PMMA film in sample (I). Then, the difference in absorption spectrum between samples (I) and (II) does not come from the pH dependence.

Table 1
Molecular parameters obtained from the E-A spectra of N719 under different sample conditions.

Sample	Peak position (nm)	A (10^{-4} MV^{-2} cm^2)	$\Delta\bar{\alpha}$ (Å^3)	$\Delta\mu$ (D)
N719 solid film (sample (I))				
Band 1	557	0	9 ± 2	7.0 ± 0.1
Band 2	408	0	0	10.0 ± 0.3
N719/TiO_2 film (sample (II))				
Band 1	543	10.3 ± 0.3	95 ± 5	11.0 ± 1.0
Band 2	398	−10.8 ± 0.8	0	20.0 ± 1.0
N719 in EtOH				
Band 1	521	–	–	–
Band 2	381	–	–	–

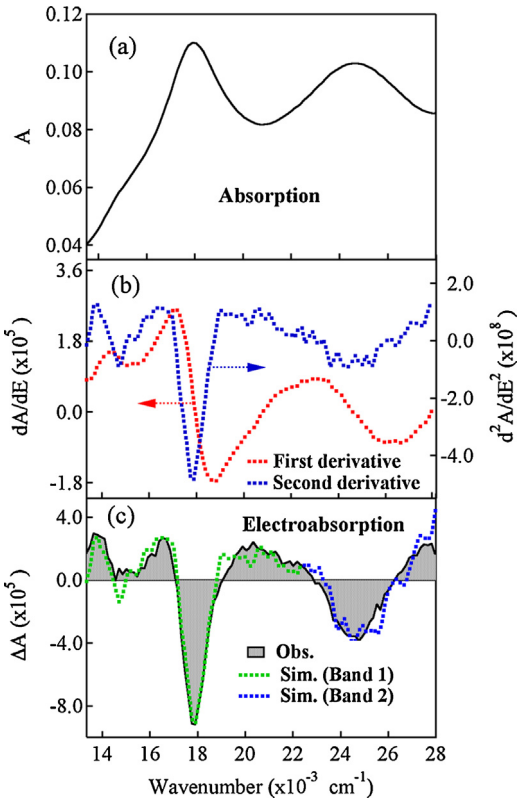

Fig. 2. (a) Absorption spectrum of N719 solid film (sample (I)), (b) the first and second derivatives of the absorption spectrum, (c) E-A spectrum (shaded line) observed with a field strength of 1.0 MV cm^{-1}, and simulated spectrum (dotted line).

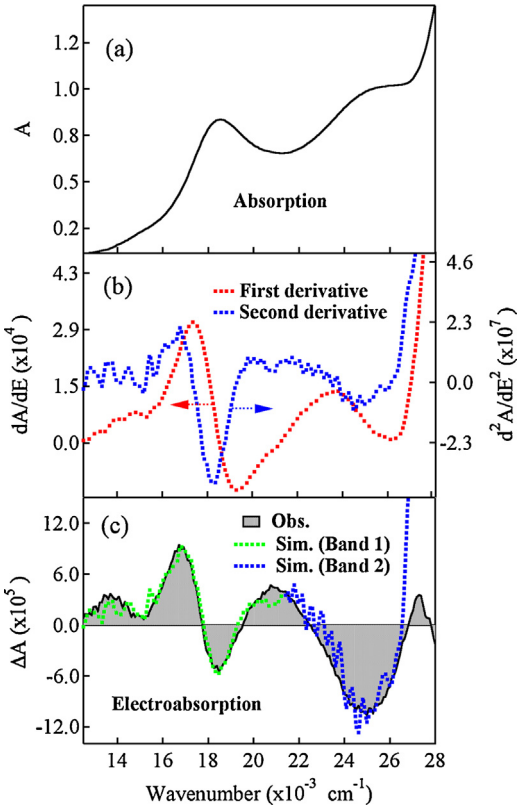

Fig. 3. (a) Absorption spectrum of N719 on TiO_2 (sample (II)), (b) the first and second derivatives of the absorption spectrum, (c) E-A spectrum (shaded line) observed with a field strength of 0.2 MV cm^{-1}, and simulated spectrum (dotted line).

Figs. 2 and 3 show the absorption and E-A spectra of N719 of sample (I) and sample (II) in the range of 14000–28000 cm^{-1}, which were obtained with a field strength of 1.0 MV cm^{-1} and 0.2 MV cm^{-1}, respectively. These E-A spectra were obtained at the magic angle of χ (=54.7°); χ is the angle between the direction of applied electric field and the electric vector of the incident light. The first and second derivatives of the absorption spectra are also shown in these figures.

In the presence of applied electric field ($\boldsymbol{F}$), the shift of the transition energy (ΔE) is related to the difference in dipole moment ($\Delta\mu$) and molecular polarizability ($\Delta\alpha$) between the excited state and the ground state; $\Delta E = -\Delta\mu \cdot F - F \cdot \Delta\alpha \cdot F/2$, where $\Delta\mu$ and $\Delta\alpha$ are given by $\mu_e - \mu_g$ and $\alpha_e - \alpha_g$, respectively, with the electric dipole moment and molecular polarizability in the ground state, i.e., μ_g, α_g, and in the excited state, i.e., μ_e, α_e. The electric field dependence of the transition moment can be written as:

$$\boldsymbol{d}^F = \boldsymbol{d} + \mathbf{X} \cdot \boldsymbol{F} + \boldsymbol{F} \cdot \mathbf{Y} \cdot \boldsymbol{F} \tag{1}$$

where $\boldsymbol{d}$ is the transition moment vector in the absence of $\boldsymbol{F}$, and $\mathbf{X}$ and $\mathbf{Y}$ are the transition moment polarizability and hyperpolarizability tensors, respectively. By assuming an isotropic distribution of the molecules in the absence of $\boldsymbol{F}$, the intensity of the E-A spectrum at wavenumber, ν, observed at the second harmonics of the modulation frequency, i.e., $\Delta A(\nu)$, is given by the following equation [28–31]:

$$\Delta A(\nu) = (fF)^2 \left[A_\chi A(\nu) + B_\chi \nu \frac{d}{d\nu} \left\{ \frac{A(\nu)}{\nu} \right\} + C_\chi \nu \frac{d^2}{d\nu^2} \left\{ \frac{A(\nu)}{\nu} \right\} \right] \tag{2}$$

where f is the internal field factor. The coefficient A_χ depends both on the field-induced change in transition moment and on the field-induced orientation. The coefficients B_χ and C_χ correspond to the spectral shift and the spectral broadening of absorption spectra, which mainly results from $\Delta\alpha$ and $\Delta\mu$, respectively, between the ground and excited states. By assuming that molecules are fixed in immobilized film, the coefficients for the magic angle of χ (=54.7°) are given as follows:

$$A_{54.7} = \frac{1}{3|\boldsymbol{d}|^2} \sum_{i,j} X_{ij}^2 + \frac{2}{3|\boldsymbol{d}|^2} \sum_{i,j} d_i Y_{ijj}^2 \tag{3}$$

$$B_{54.7} = \frac{\Delta\bar{\alpha}}{2hc} + \frac{2}{3hc|\boldsymbol{d}|^2} \sum_{i,j} d_i X_{ij} \Delta\mu_j \tag{4}$$

$$C_{54.7} = \frac{1}{6h^2c^2} |\Delta\boldsymbol{\mu}|^2 \tag{5}$$

where μ_i and d_i are the vector components of the electric dipole moment and transition moment, respectively, along the molecular axis, $\Delta\bar{\alpha}$ is the average of the trace of $\Delta\alpha$, h is Planck's constant, c is velocity of light, X_{ij} and Y_{ijk} are the tensor components of $\mathbf{X}$ and $\mathbf{Y}$, respectively. If the magnitude of $\Delta\mu$ following the optical absorption is significant, the presence of electric field will broaden an isolated transition, giving rise to the E-A spectrum, the shape of which is the second derivative of the absorption spectrum. If the magnitude of $\Delta\bar{\alpha}$ is significant, the shape of the E-A spectrum is the first derivative of the absorption spectrum, resulting from the spectral shift upon application of $\boldsymbol{F}$. The values of $|\Delta\boldsymbol{\mu}|(\equiv \Delta\mu)$ and $\Delta\bar{\alpha}$ can be obtained from the analysis of the derivative parts of the E-A spectra. It is noted that plots of the field-induced change in absorption intensity is proportional to the square of the applied field strength, as expected from Eq. (2) (see Fig. 4).

As shown in Fig. 2, the E-A spectrum of N719 of sample (I) is very similar in shape to the second derivative of the absorption spectrum of MLCT band, indicating that the field-induced change in absorption spectrum mainly come from $\Delta\mu$ following absorption to the excited states from the ground state. The fact that the

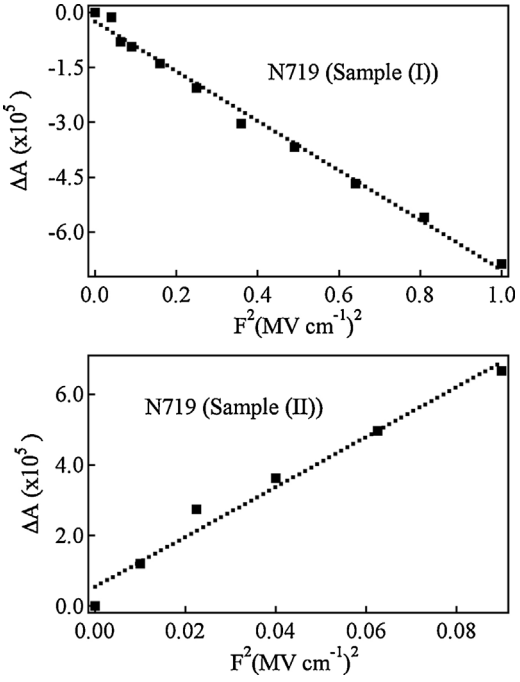

Fig. 4. Plots of the electric-field-induced change in absorption intensity of 719 as a function of the square of the applied electric field in a crystalline state, i.e., sample (I) (upper) and on the interface of TiO_2 nanocrystals, i.e., sample (II) (lower). Monitoring wavelength was 560 nm and 595 nm, respectively, where E-A signals show minimum and maximum, respectively. Dotted straight lines are guide to eyes.

zeroth derivative component is negligible in the E-A spectra of sample (I) indicates that the transition moment polarizability and hyperpolarizability are negligible in the N719 solid film. From the second derivative component of the E-A spectra, the magnitudes of $\Delta\mu$ following absorption of sample (I) have been determined to be 7.0 ± 0.1 D and 10.0 ± 0.3 D, respectively, for Bands 1 and 2. Actually, the first derivative component was necessary to reproduce the E-A spectra of Band 1, from which the magnitude of $\Delta\bar{\alpha}$ was determined to be 9.0 ± 2.0 Å^3. Note that it is assumed that the internal field factor f in Eq. (2) is unity and that the first term is dominant in Eq. (4). The fitted spectrum of sample (I) is shown in Fig. 2, together with the observed E-A spectrum. Each of the first and second derivatives of the absorption spectrum in the fitted spectrum is shown in Fig. 5 to visualize the contribution of each derivative component. It is noted that the E-A spectrum of Band 2 of sample (I) can be reproduced with only the second derivative of the absorption spectrum.

E-A spectra of N719 of sample (II) are different from those of sample (I), as shown in Fig. 3. The E-A spectra could be simulated by a combination of the zeroth, first and second derivatives of the absorption spectrum in both Bands 1 and 2. The fitted spectrum of sample (II) is shown in Fig. 3, together with the observed E-A spectrum. Each derivative component contributed to the fitted spectrum is shown in Fig. 5. From the second derivative component, the magnitudes of $\Delta\mu$ were evaluated to be 11.0 ± 1.0 D in Band 1 and 20.0 ± 1.0 D in Band 2, respectively, in sample (II) (see Table 1). Thus, the values of $\Delta\mu$ of N719 sensitized on TiO_2 are much larger than those in the solid film, indicating that the attachment of N719 to TiO_2 increases the charge transfer character of the photoexcited state. It should be stressed that the quantitative evaluation of the charge-transfer character in the photoexcited state thus obtained from the E-A measurements cannot be done by transient absorption spectroscopy and IR spectroscopy without application of electric fields. The significant contribution of the zeroth derivative component in the E-A spectra indicates that the transition moment of sample (II) is well affected by application of electric fields, resulting from the significant increase of the transition moment polarizability and/or hyperpolarizaiblity by adsorption of N719 to TiO_2 (see Eq. (3)). Unfortunately, however, each tensor component of these polarizabilities could not be deduced in the present study.

Electron injection from dye sensitizer to TiO_2 nanoparticles plays a significant role in DSSC following the charge separation in the photoexcited state. The enhanced charge-separated character of photoexcited states can be attributed to the interfacial charger transfer from N719 to TiO_2, which makes N719 a suitable dye sensitizer in DSSC because of its excellent electron injection. The present results are similar to the systems of $Fe^{II}(CN)_6^{4-}$ donor complex and coumarin-343 bound to the surface of TiO_2 [20,23].

The absorption spectrum and the alignment of ground and excited state energies investigated by the high level DFT/TDDFT calculation have been reported by Angelis et al. [19] for N719 adsorbed on TiO_2 surface, i.e., with a model of $(TiO_2)_{82}$ cluster. The visible absorption centered at around 530 nm, that is, Band 1 in the present study, was suggested to induce a strong coupling between dye and TiO_2 unoccupied levels to form the combined system's excited state, where the excited electron is already delocalized into the semiconductor. Considering the high density of unoccupied TiO_2 state in corresponding of the visible absorption band maximum and the strong coupling, an ultrafast and almost instantaneous electron injection from a nonthermalized singlet state reached by optical transition of Band 1 was predicted, in agreement with the present results.

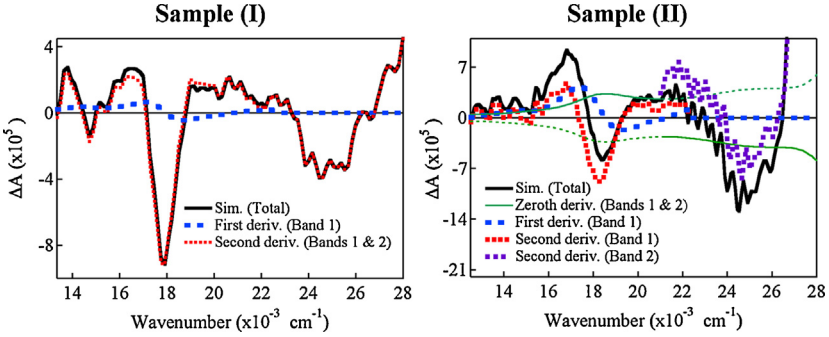

Fig. 5. (Left) The first and second derivatives of the absorption spectrum (thick broken line and thin dotted line, respectively), which contribute to the simulated E-A spectrum of sample (I) (solid line). (Right) The zeroth, first and second derivatives of the absorption spectrum (thin solid line, broken line and dotted line, respectively), which contribute to the simulated E-A spectrum of sample (II) (thick solid line). Bands 1 and 2 are separately simulated in both cases. Thin dotted line, which corresponds to the zeroth derivative components of Bands 1 and 2, respectively, is not contributed to the simulated spectrum in sample (II).

According to the calculation [19], the lowest excitation is located at 649 nm, with a sizable oscillator strength. In fact, weak absorption band is observed as a shoulder in the absorption spectrum at ca. 680 nm (ca. 14,710 cm^{-1}) in sample (I) and 660 nm (ca. 15,160 cm^{-1}) in sample (II), as shown in Figs. 1–3. The strong coupling between dye and TiO_2 was also considered in the excited state reached by absorption of this band, and an ultrafast electron injection was suggested following optical excitation of this band [19]. When the E-A spectra given in Figs. 2 and 3 are carefully watched from this point of view, it is realized that a minimum is located at 680 and 660 nm in the E-A spectra of samples (I) and (II), respectively, implying the presence of the E-A band given by the second derivative of the weak absorption band given by a shoulder, which is hereafter called as Band X. These results suggest that the change in electric dipole moment is induced by excitation of Band X, similar to Bands 1 and 2. Since the weak absorption intensity of Band X could not be determined precisely, the magnitude of $\Delta\mu$ could not be determined for Band X. As far as the second derivative of the absorption spectrum is compared with the E-A spectrum in the low wavenumber region, however, the signal intensity of the second derivative component of sample (II) looks much larger than that of sample (I). In comparison with sample (I), for example, the minimum of Band X in the second derivative spectra is not clear in sample (II), whereas the minimum is so clear in the E-A spectrum, implying that the magnitude of $\Delta\mu$ of Band X in sample (II) is larger than the corresponding one in sample (I), as in the case of Bands 1 and 2. With excitation at Band X, therefore, the excited electron is considered to be delocalized into the semiconductor, as suggested by the theoretical calculation [19]. Thus, a fast electron injection is considered to occur directly from the state reached by optical excitation, irrespective of the excited bands.

The E-A spectra of alizarin, which can be served as a light absorber in model systems designed for the new type solar cells, were reported both free in solution and adsorbed to TiO_2 nanoparticles [21]. The aim of the experiments was to examine whether the electronic distribution of the photoexcited alizarin/TiO_2 extends into the solid and involves the contribution of the Ti atom or it remains localized within the alizarin molecules. The results were obtained that the magnitude of $\Delta\mu$ of alizarin adsorbed on TiO_2 was much larger than that of the free molecules in ethanol solution, similar to the present results of the N719/TiO_2 system. However, the large value of $\Delta\mu$ of adsorbed alizarin was explained by the interaction of the adsorbed dye with the electric field generated by charged nanoparticles, not by the alizarin-to-TiO_2 charge transfer character. In the present results, it is also necessary to consider the internal electric field effect of TiO_2, because the internal field factor f was assumed to be unity to determine the magnitudes of $\Delta\mu$ and $\Delta\tilde{\alpha}$. As shown in Fig. 1 and Table 1, the absorption spectrum of the N719/TiO_2 film exhibited a blue-shift in comparison with the spectrum of the N719 solid film, i.e., sample (I), suggesting that the local field of TiO_2 is smaller than that of N719 crystals. Therefore, it is unlikely that the present result that $\Delta\mu$ of the N719/TiO_2 film is much larger than that of N719 solid film comes from the local field effect. As already mentioned, the electron injection occurs following photoexcitation of the locally excited state of the dyes which acquire interfacial charge transfer state character through binding of N719 to TiO_2 surface. The fact that the electric field effect on transition moment is very significant for N719 adsorbed on TiO_2, but not for N719 solid film, also indicates the strong interaction between N719 and TiO_2 on the N719/TiO_2 interface.

Acknowledgement

This work was supported by the JST-NSC cooperative research project between Japan and Taiwan (NSC 99-2923-M-001-MY3).

References

[1] B. O'Regan, M. Grätzel, A low-cost, high-efficiency solar cell based on dye-sensitized colloidal TiO_2 films, Nature 353 (1991) 737–740;
M. Grätzel, Photoelectrochemical cells, Nature 414 (2001) 338–344;
M. Grätzel, Dye-sensitized solar cells, J. Photochem. Photobiol. C 4 (2003) 145–153.
[2] Q. Wang, S. Ito, M. Grätzel, F. Fabregat-Santiago, I. Mora-Seró, J. Bisquert, T. Bessho, H. Imai, Characteristics of high efficiency dye-sensitized solar cells, J. Phys. Chem. B 110 (2006) 25210–25221.
[3] C.-Y. Chen, S.-J. Wu, J.-Y. Li, C.-G. Wu, J.-G. Chen, K.-C. Ho, A new route to enhance the light-harvesting capability of ruthenium complexes for dye-sensitized solar cells, Adv. Mater. 19 (2007) 3888–3891.
[4] Q. Yu, Y. Wang, Z. Yi, N. Zu, J. Zhang, M. Zhang, P. Wang, High-efficiency dye-sensitized solar cells: the influence of lithium ions on exciton dissociation, charge recombination, and surface states, ACS Nano 4 (2010) 6032–6038.
[5] W.-K. Huang, C.-W. Cheng, S.-M. Chang, Y.-P. Lee, E.W.-G. Diau, Synthesis and electron-transfer properties of benzimidazole-functionalized ruthenium complexes for highly efficient dye-sensitized solar cells, Chem. Commun. 46 (2010) 8992–8994.
[6] G.C. Vougioukalakis, A.I. Philippopoulos, T. Stergiopoulos, P. Falaras, Contributions to the development of ruthenium-based sensitizers for dye-sensitized solar cells, Coord. Chem. Rev. 255 (2011) 2602–2621.
[7] L. S-Mende, U. Bach, R. H-Baker, T. Horiuchi, H. Miura, S. Ito, S. Uchida, M. Gratzel, Organic dye for highly efficient solid-state dye-sensitized solar cells, Adv. Mater. 17 (2005) 813–815.
[8] G. Zhang, H. Bala, Y. Cheng, D. Shi, X. Lv, Q. Yu, P. Wang, High efficiency and stable dye-sensitized solar cells with an organic chromophore featuring a binary π-conjugated spacer, Chem. Commun. (2009) 2198–2200.
[9] W. Zeng, Y. Cao, Y. Bai, Y. Wang, Y. Shi, M. Zhang, F. Wang, C. Pan, P. Wang, Efficient dye-sensitized solar cells with an organic photosensitizer featuring orderly conjugated ethylenedioxythiophene and dithienosilole blocks, Chem. Mater. 22 (2010) 1915–1925.
[10] C.-P. Hsieh, H.-P. Lu, C.-L. Chiu, C.-W. Lee, S.-H. Chuang, C.-L. Mai, W.-N. Ywn, S.-J.E. Hsu, W.-G. Diau, C.-Y. Yeh, Synthesis and characterization of porphyrin sensitizers with various electron-donating substituents for highly efficient dye-sensitized solar cells, J. Mater. Chem. 20 (2010) 1127–1134.
[11] A. Yella, H.W. Lee, H.N. Tsao, C. Yi, A.K. Chandiran, M.K. Nazeeruddin, E.W.G. Diau, C.Y. Yeh, S.M. Zakeeruddin, M. Grätzel, Porphyrin-sensitized solar cells with cobalt (II/III)–based redox electrolyte exceed 12 percent efficiency, Science 334 (2011) 629–634.
[12] M.K. Nazeeruddin, F. De Angelis, S. Fantacci, A. Selloni, G. Viscardi, P. Liska, S. Ito, B. Takeru, M. Grätzel, Combined experimental and DFT-TDDFT computational study of photoelectrochemical cell ruthenium sensitizers, J. Am. Chem. Soc. 127 (2005) 16835–16847.
[13] S. Ardo, G.J. Meyer, Photodriven heterogeneous charge transfer with transition-metal compounds anchored to TiO_2 semiconductor surfaces, Chem. Soc. Rev. 38 (2009) 115–164.
[14] T. Hannappel, B. Burfeindt, W. Storck, F. Willig, Measurement of ultrafast photoinduced electron transfer from chemically anchored Ru-dye molecules into empty electronic estates in a colloidal anatase TiO_2 film, J. Phys. Chem. B 101 (1997) 6799–6802.
[15] G. Benko, J. Kallioinen, J.E.I. Kotppi-Tommola, A.P. Yartsev, V. Sundström, Photoinduced ultrafast dye-to-semiconductor electron injection from non-thermalized and thermalized donor states, J. Am. Chem. Soc. 124 (2002) 489–493.
[16] B. Wenger, M. Grätzel, J.-E. Moser, Rationale for kinetic heterogeneity of ultrafast light-induced electron transfer from Ru(II) complex sensitizers to nanocrystalline TiO_2, J. Am. Chem. Soc. 127 (2005) 12150–12151.
[17] H. Gerischer, Charge transfer processes at semiconductor-electrolyte interfaces in connection with problems of catalysis, Surf. Sci. 18 (1969) 97–122.
[18] F. De Angelis, S. Fantacci, A. Selloni, M.K. Nazeeruddin, M. Grätzel, First-principles modeling of the adsorption geometry and electronic structure of Ru(II) dyes on extended TiO_2 substrates for dye-sensitized solar sell applications, J. Phys. Chem. C 114 (2010) 6054–6061.
[19] F. De Angelis, S. Fantacci, E. Mosconi, M.K. Nazeeruddin, M. Grätzel, Absorption spectra and excited state energy levels of the N719 dye on TiO_2 in dye-sensitized solar cell models, J. Phys. Chem. C 115 (2011) 8825–8831.
[20] M. Khoudiakov, A.R. Parise, B.S. Brunschwig, Interfacial electron transfer in $Fe^{II}(CN)_6^{4-}$–sensitized TiO_2 nanoparticles: a study of direct charge injection by electroabsorption spectroscopy, J. Am. Chem. Soc. 125 (2003) 4637–4642.
[21] A. Nawrocka, S. Krawczk, Electronic excited state of alizarin dye adsorbed on TiO_2 nanoparticles: a study by electroabsorption (Stark effect) spectroscopy, J. Phys. Chem. C 112 (2008) 10233–10241.
[22] A. Nawrocka, A. Zdyb, S. Krawczyk, Stark spectroscopy of charge-transfer transitions in catechol-sensitized TiO_2 nanoparticles, Chm. Phys. Lett. 475 (2009) 272–276.
[23] K.A. Walters, D.A. Gaal, J.T. Hupp, Interfacial charge transfer and colloidal semiconductor dye-sensitization: mechanism assessment via Stark emission spectroscopy, J. Phys. Chem. B 106 (2002) 5139–5142.
[24] U.B. Cappel, S.M. Feldt, J. Schoneboom, A. Hagfeldt, G. Boschloo, The influence of local electric fields on photoinduced absorption in dye-sensitized solar cells, J. Am. Chem. Soc. 132 (2010) 9096–9101.

[25] S. Ardo, Y. Sun, F.N. Castellano, G.J. Meyer, Excited-state electron transfer from ruthenium-polypyridyl compounds to anatase TiO_2 nanocrystallites: evidence for a Stark effect, J. Phys. Chem. B 114 (2010) 14596–14604.
[26] M. Pastore, F.D. Angelis, Computational modeling of Stark effects in organic dye-sensitized TiO_2 heterointerfaces, J. Phys. Chem. Lett. 2 (2011) 1261–1267.
[27] E. Jalviste, N. Ohta, Stark absorption spectroscopy of indole and 3-methylindole, J. Chem. Phys. 121 (2004) 4730–4739.
[28] W. Liptay, in: E.C. Lim (Ed.), Excited States, vol. 1, Academic, New York, 1974, p. 129.
[29] G.U. Bublit, S.G. Boxer, Stark spectroscopy: applications in chemistry, biology, and materials science, Annu. Rev. Phys. Chem. 48 (1997) 213–242.
[30] S.A. Locknar, A. Chowdhury, L.A. Peteanu, Matrix and temperature effects on the electronic properties of conjugated molecules: an electroabsorption study of all-trans-retinal, J. Phys. Chem. B 104 (2000) 5816–5824.
[31] E. Jalviste, N. Ohta, Theoretical foundation of electroabsorption spectroscopy: self-contained derivation of the basic equations with the direction cosine method and the Euler angle method, J. Photochem. Photobiol. C: Photochem. Rev. 8 (2007) 30–46.